

# Metabonomic Characterization of The Low-grade Human Astrocytomas and Meningiomas Using Magic-angle Spinning $^1\text{H}$ Nuclear Magnetic Resonance Spectroscopy and Principal Component Analysis\*

CHEN Wen-Xue<sup>1,2</sup>, LOU Hai-Yan<sup>3,4</sup>, ZHANG Hong-Ping<sup>5</sup>, NIE Xiu<sup>6</sup>, XIANG Yun<sup>1,2</sup>, YANG Yong-Xia<sup>1,2</sup>,  
WU Guang-Yao<sup>1,5</sup>, QI Jian-Pin<sup>3</sup>, YUE Yong<sup>1</sup>, LEI Hao<sup>1</sup>, TANG Hui-Ru<sup>1\*\*</sup>, DENG Feng<sup>1\*\*</sup>

<sup>1</sup> State Key Laboratory of Magnetic Resonance and Atomic and Molecular Physics, Wuhan Institute of Physics and Mathematics, The Chinese Academy of Sciences, Wuhan 430071, China; <sup>2</sup> Graduate School of The Chinese Academy of Sciences, Beijing 100049, China;

<sup>3</sup> Tongji Hospital, Tongji Medical College, Huazhong University of Science and Technology, Wuhan 430022, China;

<sup>4</sup> The First Affiliated Hospital, College of Medicine, Zhejiang University, Hangzhou 310003, China;

<sup>5</sup> Zhongnan Hospital, Medical College, Wuhan University, Wuhan 430071, China;

<sup>6</sup> Union Hospital, Tongji Medical College, Huazhong University of Science and Technology, Wuhan 430022, China)

**Abstract** Metabolic characteristics of 39 human brain tumor tissues, including 15 astrocytomas, 13 fibroblastic meningiomas and 11 transitional meningiomas from 39 individual patients, have been studied using high resolution magic-angle spinning (HRMAS)  $^1\text{H}$  NMR spectroscopy in conjunction with principal component analysis (PCA). With rich metabolite information,  $^1\text{H}$  NMR spectra showed that the tumor-tissue metabonome was dominated by lipids, lactate, *myo*-inositol, creatine, choline metabolites such as choline, phosphocholine and glycerophosphocholine, amino acids such as alanine, glutamate, glutamine, taurine, N-acetyl-aspartate and glutathione. PCA of the tumor NMR spectra clearly showed metabonomic differences between low-grade astrocytomas and meningiomas whereas such differences were more moderate between fibroblastic and transitional meningiomas. Compared with meningiomas, the low-grade astrocytomas had higher levels of glycerophosphocholine, phosphocholine, *myo*-inositol and creatine but lower levels of alanine, glutamate, glutamine, glutathione and taurine. The N-acetyl-aspartate level was low but detectable in low-grade astrocytomas whereas it was not detectable in meningiomas. It is concluded that tissue metabonomics technology consisting of HRMAS  $^1\text{H}$  NMR spectroscopy and multivariate data analysis (MVDA) offers a useful tool (1) for distinguishing different types of brain tumors, (2) for providing the metabolic information for human brain tumors, which are potentially useful for understanding biochemistry of tumor progression.

**Key words** human brain tumor, glioma, astrocytomas, meningioma, high resolution magic-angle spinning (HRMAS) nuclear magnetic resonance spectroscopy, pattern recognition, statistical analysis.

Gliomas and meningiomas are the most frequently encountered human brain tumors<sup>[1]</sup> and the clinical survival rates among brain tumor patients vary considerably depending on the type and grade of tumors<sup>[2]</sup>. Gliomas include astrocytic, oligodendroglial, ependymal and neuronal tumours whereas meningiomas have many subtypes such as meningothelial, fibroblastic (fibrous), transitional (mixed), and psammomatous meningiomas. Clear understandings of the metabolic biochemistry of the

tumors are vitally important to aid more accurate diagnosis and prognosis which in turn can help

\*This work was supported by grants from The National Natural Science Foundation of China (10234070, 20573132 and 20575074) and The Chinese Academy of Sciences (100T programme: T12508-06S138).

\*\*Corresponding author. Tel: 86-27-87198430, 87198820

TANG Hui-Ru. E-mail: Huiru.Tang@wipm.ac.cn

DENG Feng. E-mail: Dengf@wipm.ac.cn

Received: January 28, 2008 Accepted: April 15, 2008

therapeutic planning and potentially improve the clinical outcome<sup>[3,4]</sup>. At present, some modern imaging methods, such as magnetic resonance imaging (MRI), X-ray computed tomography (CT), and positron-emission tomography (PET), provide useful information<sup>[5~8]</sup> on tumor mass and location, they remain to be complementary in the clinical settings since they can only provide limited information for a precise classification and diagnosis. The ultimate clinical diagnosis of brain tumors relies, almost exclusively, on histopathological evaluation of tumor biopsy. Given the heterogeneity of some tumor tissues, however, the histopathological evaluation normally takes only a small part of the tumor and may not adequately represent the total tumor property<sup>[9]</sup>. Such approach is also effective only when tissue or cellular morphological changes reach certain scale, being of limited values for early diagnosis even though such early diagnosis may be vitally important for early intervention and improvement of patient survival. Furthermore, the histopathological evaluation is generally time consuming requiring as much time as about 24 hours for tissue fixation and microscopic assessment. The frozen section technique requires half an hour but generally can only provide low diagnostic accuracy<sup>[10]</sup>. Sometimes the method is also subjected to experience of the pathologists. Moreover, histopathological methods conceivably provide little or no metabolite information for the tumors even though such information may be important for prognosis and understanding the underlying molecular events related to the carcinogenesis and developments. Complimentary methods have long been in demand to extract further information especially in terms of metabolic characteristics of the tumors compared with normal tissues.

*In vivo* <sup>1</sup>H magnetic resonance spectroscopy (MRS) and *in vitro* <sup>1</sup>H nuclear magnetic resonance (NMR) spectroscopy of the tissue extracts have provided more information on metabolites correlated with histopathology of tissue specimens and helped to improve understandings of tumor biochemistry which is beneficial to the diagnostic accuracy of human brain tumors<sup>[11~13]</sup>. Although *in vivo* <sup>1</sup>H MRS is the only non-invasive *in vivo* metabolite detection methods, this method often detects only a few metabolites such as lipids, total creatine (tCre), total choline (tCho), lactate (Lac), glutamate and glutamine (Glx), alanine (Ala) and N-acetyl-aspartate (NAA) owing to its limited

spectral resolution and detection sensitivity. The spectral baseline and signal-to-noise ratio were not always good enough for quantitative or pattern recognition analysis. Furthermore, the detectable metabolite signals were often not unambiguously resolved. For example, signals of choline, phosphocholine and glycerophosphocholine were often collectively reported as so-called “total choline (tCho)”. Similarly, creatine and phosphocreatine signals were collectively reported as “total creatine (tCre)”. The signals for glutamate and glutamine were often reported together as GLX though the functions of these metabolites were not necessarily the same. The signals of lactate and lipids or alanine and lipids at  $\delta$  1.2 ~ 1.5 were not clearly resolved under normal short echo MRS experiments and they have to be resolved with medium or long echo experiments<sup>[11]</sup> which invert the doublets of lactate and alanine, being difficult for quantitative analysis. Even more importantly, when the changes of these overlapping metabolites were not following the same trend, signal average in the overlapped signals, for example, by compensation from each other, can lead to mistakes as constant. On the other hand, the *in vitro* <sup>1</sup>H NMR spectroscopic methods, though having much higher resolution, require solvent extraction of tissues, leading to the loss of the vitally important compartmentation information. Furthermore, the extraction procedures were often laborious and may suffer from possible chemical changes for the metabolites and incompleteness of extraction.

More recently, high resolution magic-angle spinning (HRMAS) NMR spectroscopy has emerged as an ideal tool for studying tissue metabolism. With the requirement of small amount of tissue samples (ca. 10 mg) and little or no sample preparation, HRMAS methods offer direct analysis of the metabolite composition (i.e, metabonome) of the intact biological tissues<sup>[14~16]</sup> and high spectral resolution that is close to solution state NMR. Therefore, such methods have already been widely used in studying the metabolism of liver<sup>[17]</sup>, kidney<sup>[18]</sup> and brain tissues<sup>[19]</sup> of animal models and biopsy of human liver<sup>[20]</sup>, breast ductal<sup>[21]</sup>, prostate<sup>[22]</sup> and brain<sup>[14]</sup> tissues. In particular, when used in conjunction with multivariate data analysis (MVDA) based pattern recognition (PR) methods, such as principal components analysis (PCA), the methods have become an important part of *ex vivo* tissue metabonomics platform, which is the

only known non-destructive tissue metabonomics technique for the time being. These advantages have already been exploited<sup>[23~26]</sup> to provide a convenient, rapid and accurate complementary method for biochemistry studies, diagnosis, classification and grading of human brain tumors.

Some studies have already been conducted for human brain tumors, such as glioma and meningioma, using *in vivo* MRS and *in vitro* NMR. Even with the aforementioned drawbacks, these studies have shown effectiveness in differentiating normal human brain from various tumor<sup>[27~32]</sup> and differentiating high-grade glioma from meningioma<sup>[11, 33~36]</sup>. *In vivo* MRS studies have also showed metabolic differences between human low-grade glioma and meningioma in the levels of total-choline, alanine, *myo*-inositol, total-creatine<sup>[11, 27]</sup>, lactate<sup>[27]</sup>, Glx (i.e., glutamate and glutamine)<sup>[11, 27, 37]</sup>, and glutathione<sup>[37]</sup>. However, no significant differences were reported on lipid under MRS conditions. For animal models, *in vivo* MRS studies of rats<sup>[38]</sup> at 9.4T showed more metabolites including taurine, *scyllo*-inositol, aspartate,  $\gamma$ -aminobutyric acid, N-acetylaspartylglutamate though choline metabolites remained unresolved. *In vitro* <sup>1</sup>H NMR spectroscopy of the tissue extracts showed that only the levels of alanine and glutamate as well as ratios for glycine/creatine, alanine/creatine and total-choline/creatine had significant difference ( $P < 0.05$ ) between low-grade gliomas and meningiomas<sup>[13, 31, 39]</sup>. No significant differences were reported on taurine, *myo*-inositol and creatine though meningiomas had higher level of taurine<sup>[31]</sup>, and lower levels of *myo*-inositol<sup>[13, 31, 39, 40]</sup> and creatine<sup>[31, 39, 40]</sup> compared with low-grade glioma. No information was reported on the lipid levels either probably due to the method limitation.

Some preliminary results of the HRMAS NMR studies on glioma and meningioma showed significant difference ( $P < 0.05$ ) in the level of glutamate and ratios of glycine/creatine, alanine/creatine and glutamate/creatine<sup>[14, 41]</sup>. Whilst these studies reported important findings, both studies were based on some limited patients including two low-grade astrocytomas and six meningiomas<sup>[14]</sup> in one study and one low-grade astrocytoma and one meningioma in another<sup>[41]</sup>. Therefore, further conformational studies with more cases are required.

When more cases are studied, simple spectra comparisons will not be adequate enough to obtain all

useful information on tissue metabonomic changes due to the spectral complexity and large quantity of data. Multivariate data analysis based pattern recognition is expected to be much more effective in these cases and such studies on brain tumor metabonomic characteristics are not available for the time being. There are also no HRMAS NMR studies reported, so far, on the metabolic differences between the subtypes of meningiomas, such as fibroblastic and transitional meningiomas. Furthermore, it is not certain whether metabolite levels other than those reported are also different between low-grade glioma and meningiomas when more cases are studied.

In this study, HRMAS <sup>1</sup>H NMR methods are employed in combination with principal components analysis (PCA) to analyse the metabonomic characteristics of 39 human brain tumor samples with the aims (1) to understand the metabolic characteristics of the low-grade astrocytomas and meningiomas with more samples, and metabonomic differences between fibroblastic and transitional meningiomas, (2) to explore the feasibility of metabonomics technology as a complimentary tool for understanding the relevant biochemical processes accompanied with carcinogenesis and development to provide possible assistant for the classification of human brain tumors.

## 1 Materials and methods

### 1.1 Collection of brain tissue specimens

39 human brain tumor specimens were obtained from 39 patients at the Department of Neurosurgery, Tongji and Union Hospital, Tongji College of Medicine, Huazhong University of Science and Technology, and at the Department of Neurosurgery, Zhongnan Hospital, Medical College of Wuhan University. All tissue samples used for MAS studies were dissected from specimens used for clinical pathology evaluations and this study was reviewed and approved by the local ethics committee. The tumor samples studied include 15 astrocytomas from 12 male and 3 female patients aged between 21 and 63, 13 fibroblastic meningiomas from 5 male and 8 female aged at 16~60 and 11 transitional meningiomas from one male and 10 female patients aged at 25~66. All samples were snap-frozen in liquid nitrogen after craniotomy and the whole sample collection process normally took no more than 30 min. All snap-frozen samples were stored in a freezer at  $-80^{\circ}\text{C}$  until further analysis.

## 1.2 Histopathological assessment

All samples used for histopathological examination were fixed in 10% neutral buffered formalin and routine methods were employed for histopathology studies. The tissue cross-sections, 5  $\mu\text{m}$  in thickness, were stained with Hematoxylin and Eosin (H&E) method followed with microscopic evaluation by pathologists. The diagnosis criteria were according to the 2000 revised world health organization (WHO) classification for brain tumors. With limited cases and for the sake of clarity, we classified grade I and grade II astrocytoma as low-grade astrocytoma.

## 1.3 High resolution magic-angle spinning(HRMAS) $^1\text{H}$ NMR spectroscopy

Individual tumor samples (20~30 mg) were respectively placed into a 4 mm quartz rotor specially designed for HRMAS spectroscopy after rinsed in  $\text{D}_2\text{O}$  saline at low temperature ( $4^\circ\text{C}$ ), the total sample preparation time for each sample prior to NMR detection was less than 5 min. All HRMAS  $^1\text{H}$  NMR spectra were acquired on a Varian INVOA 600 MHz spectrometer equipped with a standard gHX Nanoprobe with a spin rate of 2 kHz (due to hardware restriction). Two  $^1\text{H}$  NMR spectra for each sample were recorded using one dimensional single-pulse sequence and standard Carr-Purcell-Meiboom-Gill (CPMG) spin-echo pulse sequence [RD  $-90^\circ -(\tau - 180^\circ - \tau)n - \text{ACQ}$ ]. Water signal was pre-saturated in both cases with a weak continuous wave irradiation on water resonance during recycle delay (RD)<sup>[14, 23]</sup>. The  $90^\circ$  pulse length was adjusted to 4.2~5.7  $\mu\text{s}$  for each sample individually and typically 128 transients were collected into 16 k data with a recycle delay of 2 s and a spectral width of 12 kHz. In the case of CPMG experiment, a total spin-spin relaxation delay,  $2n\tau$  ( $\tau = 240 \sim 250 \mu\text{s}$ ), of 32 ms was used for all samples. The total acquisition time for each sample was less than 20 min. Sample temperature in the rotor was calibrated to be  $(298 \pm 1)$  K using methanol method<sup>[42,43]</sup> when the temperature controller showed 298 K.

The free induction decays (FID) were multiplied by an exponential window function with line broadening factor of 1 Hz prior to Fourier transformation (FT). All spectra were manually phase- and baseline-corrected using the software XWINNMR2.0 (Bruker Analytik, Germany) following converting data into the correct format. The proton chemical shifts were referenced internally to the centre

of the lactate methyl doublet (1.33).

$^1\text{H}$ - $^1\text{H}$  TOCSY HRMAS 2D NMR spectra were acquired on selected tumor samples for spectral assignment purpose using MLEV17 spin-lock duration of 90 ms and relaxation delay of 1 s. 2 k data points were collected over 7 200 Hz spectral width with sixteen transients averaged for each of the 256 increments. Total acquisition time was about 7.5 h. Data were zero filled to a  $4\ 096 \times 512$  matrix and weighted with a shifted square sine bell function prior to Fourier transformation in both dimensions.

The average spectra for each group of tumor samples were obtained in the following way. The spectral region  $\delta$  0.50~4.50 was divided into 4 000 buckets with a uniform width of 0.001. The integral of each bucket was then normalized to the total integrals over the entire region ( $\delta$  0.50~4.50). Such normalized spectra of each sub-group tumors were averaged numerically.

## 1.4 Principal components analysis (PCA)

Due to the presence of the spinning sidebands resulting from hardware restriction of the spinning rate to 2 kHz and relatively less signals in the aromatic region, only the signals over the range of  $\delta$  0.50~4.50 were selected for pattern recognition analysis. Each sub-spectrum was divided into 200 regions with a uniform width of 0.02. The signal intensities in each region were integrated, and each integrated region was normalized by the sum of all integrals over the entire sub-spectrum. Principal components analysis (PCA) was carried out with mean-center scaling, using the software Simca-P 10.0 (Umetrics, Sweden). Processed data were visualized by scores plots and loadings plots, where each point on the scores plot represented the metabonome of an individual sample while each point on the loadings plots represented a single spectral region (or chemical shift) contributing to the separation.

## 1.5 Conventional statistical analysis

As the absolute concentration for metabolites is difficult to quantify in the HRMAS NMR spectra without internal references, the relative concentration of the metabolites was determined in this study as the ratio of the metabolite signal integrals over that of the total spectra. Therefore, every NMR peak was normalized to the sum of the total spectrum and the data were used for statistical analysis.

The normalized integrals of metabolites and the integral ratios of the metabolites to choline(at  $\delta$  3.20)

were subjected to two-tailed student's *t*-test for 39 human brain tumors (15 low-grade astrocytomas, 13 fibroblastic and 11 transitional meningiomas) using the statistical software SPSS 10.0 (Statistical Package for Social Science, SPSS Inc). When  $P < 0.05$ , the changes of metabolite levels were considered to be statistically significant.

## 2 Results

### 2.1 Histopathological assessment of tumor samples

With histopathological evaluations, all 39 tumor samples studied here were classified into 3 groups, namely, low-grade astrocytoma, fibroblastic meningioma and transitional meningioma (Table 1).

**Table 1 Data for human brain tumor samples studied in this work**

Patient No.	Histopathological diagnosis	Grade	Gender	Age
1	Astrocytoma	II	M	32
2	Astrocytoma	II	M	48
3	Astrocytoma	II	F	36
4	Astrocytoma	II	M	38
5	Astrocytoma	II	M	46
6	Astrocytoma	II	F	35
7	Astrocytoma	II	M	22
8	Astrocytoma	II	F	32
9	Astrocytoma	II	M	32
10	Astrocytoma	I	M	63
11	Astrocytoma	II	M	58
12	Astrocytoma	I	M	63
13	Astrocytoma	I	M	39
14	Astrocytoma	II	M	21
15	Astrocytoma	II	M	33
16	Fibroblastic meningioma	I	F	50
17	Fibroblastic meningioma	I	M	26
18	Fibroblastic meningioma	I	F	52
19	Fibroblastic meningioma	I	F	60
20	Fibroblastic meningioma	I	F	48
21	Fibroblastic meningioma	I	F	55
22	Fibroblastic meningioma	I	M	51
23	Fibroblastic meningioma	I	M	16
24	Fibroblastic meningioma	I	F	51
25	Fibroblastic meningioma	I	F	16
26	Fibroblastic meningioma	I	M	37
27	Fibroblastic meningioma	I	M	40
28	Fibroblastic meningioma	I	F	33
29	Transitional meningioma	I	F	35
30	Transitional meningioma	I	M	25
31	Transitional meningioma	I	F	66
32	Transitional meningioma	I	F	43
33	Transitional meningioma	I	F	48
34	Transitional meningioma	I	F	62
35	Transitional meningioma	I	F	52
36	Transitional meningioma	I	F	42
37	Transitional meningioma	I	F	55
38	Transitional meningioma	I	F	50
39	Transitional meningioma	I	F	42

Figure 1 showed some examples of these results for the tumor tissues from two astrocytomas (grade I and II) and two meningiomas (fibroblastic and transitional). The grade I astrocytoma (Figure 1a) showed slight increase in the number of tumor cells compared with normal tissues. In contrast, grade II astrocytoma shown in Figure 1b had clear increase in the number of tumor cells with enlarged nuclei with no mitosis observed. The tumor of transitional meningioma (Figure 1c) contained both meningothelial and fibrous meningiomas which had transitional feature between them. Cellular whorls were also clearly observable. The tumor cells of fibrous meningioma (Figure 1d) were spindle-shaped resembling fibroblasts. Although the ages of these patients (Table 1) ranged from 16 to 66, no obvious age related predilection was observable here. To obtain metabolic information for these tumor tissues *ex vivo*, high resolution magic-angle spinning  $^1\text{H}$  NMR spectroscopic studies were conducted on all tissues.

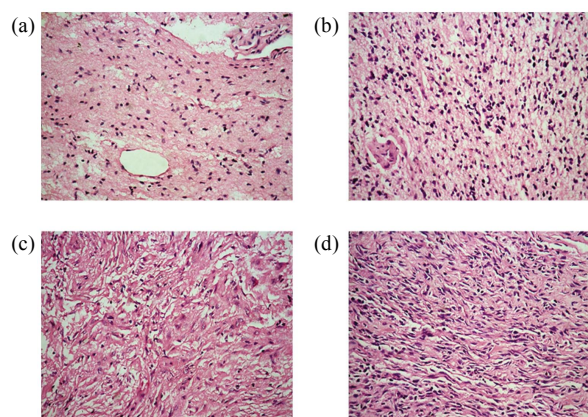


**Fig. 1 Histopathological micrographs (H&E stain) of tumor tissue with the magnification of 200**

(a) An astrocytoma (grade I ). (b) A fibrillary astrocytoma (grade II ). (c) A transitional meningioma. (d) A fibroblastic meningioma.

### 2.2 High resolution magic-angle spinning $^1\text{H}$ NMR spectroscopy

Two separate 1D  $^1\text{H}$  NMR spectra were acquired for each sample as the single-pulsed acquisition and T2-edited ones which will be denoted as CPMG spectra in the following discussion. With attenuation of the overwhelming lipid signals, the CPMG spectra showed more metabolite signals as in other reported cases<sup>[4,44]</sup>. When multiple tissue samples are employed, small differences may be present between spectra in

the same sample group due to differences in individuals and sometime inconsistency of sampling sites. The average spectra from a number of samples in the same group are conceived to have better representation for the metabolite composition of that particular group. Figure 2 showed the average HRMAS  $^1\text{H}$  NMR spectra of human brain tumor tissues from 15 low-grade astrocytomas (a), 13

fibroblastic meningiomas (b) and 11 transitional meningiomas (c) recorded with the CPMG pulse sequence at a spinning rate of 2 kHz. Apart from the intense signals of fatty acids which could not be completely suppressed by the CPMG pulse sequence due to short relaxation time (32 ms), a number of metabolite resonances were detected from three types of tumors.

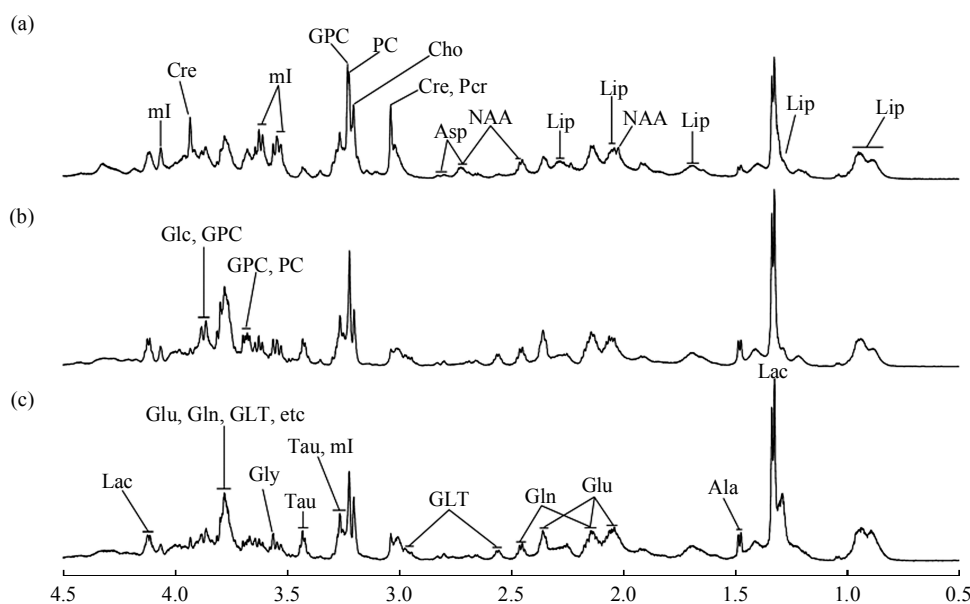


**Fig. 2** Average HR-MAS  $^1\text{H}$  NMR spectra of 39 human brain tumors acquired from CPMG pulse sequence  
(a) Low-grade astrocytomas. (b) Fibroblastic meningiomas. (c) Transitional meningiomas.

They were assigned (Table 2) based on the previously published data [13~15, 45] and  $^1\text{H}$ - $^1\text{H}$  TOCSY HRMAS 2D NMR spectra (data not shown), including choline metabolites, such as choline (Cho), phosphocholine (PC) and glycerophosphocholine (GPC), amino acids including alanine, glycine, glutamate, glutamine, leucine, isoleucine, lysine, threonine, taurine, glutathione, lactate, creatine, *myo*-inositol,  $\alpha$ -glucose and  $\beta$ -glucose. By simple visual inspection, a number of differences are observable between the spectra of low-grade astrocytomas and meningiomas. The N-acetyl-aspartate (NAA,  $\delta$  2.02) signals were low but detectable in the low-grade astrocytomas (Figure 2a) whereas no NAA was detectable in meningiomas (Figure 2b, 2c). In addition, low-grade astrocytomas contained lower

levels of glutathione, glutamate, alanine, lactate, and taurine together with high level of creatine and *myo*-inositol than meningiomas. In the present study, higher levels of PC and GPC were observed in low-grade astrocytomas than in meningiomas. Signals for glutamine and glutamate are also completely resolved and therefore can be considered separately. Lactate, alanine and lipids were well resolved in our HRMAS NMR spectra. Intense signals of glycine (Gly,  $\delta$  3.56) were detected in 17 cases of meningiomas and 5 cases of low-grade astrocytomas.

However, the complexity of spectra and large number of samples make it extremely difficult to analyse all cases as a whole just by visual inspection; multivariate data analysis is required to obtain a general differences between different tumor samples.

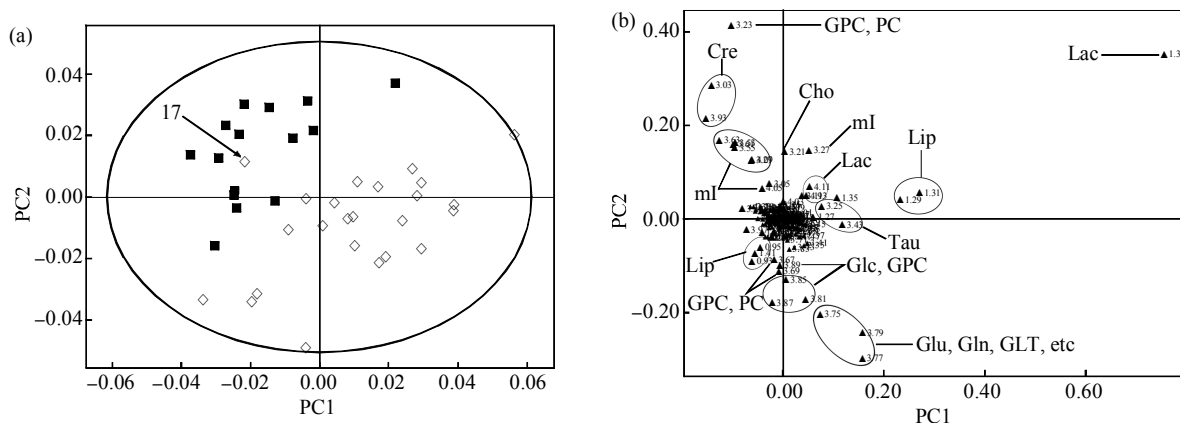
**Table 2** NMR data for the metabolites of human brain tumors

Number	Abbr.	Metabolite	$\delta$ <sup>1</sup> H (Multiplicity)
1	Ace	Acetate	1.91(s)
2	NAA	N-Acetylaspartate	2.02(s), 2.68(dd)
3	Ala	Alanine	1.48(d), 3.79(q)
4	Asp	Aspartate	2.67(dd), 2.82(dd)
5	Cho	Choline	3.20(s), 4.06(m)
6	Cre	Creatine	3.04(s), 3.93(s)
7	Iso	Isoleucine	0.95(t), 1.01(d), 1.98(m), 3.69(d)
8	Glc	$\alpha$ -Glucose	3.41(t), 3.71(t), 3.84(m), 5.23(d)
9	Glc	$\beta$ -Glucose	3.40(t), 3.72(dd), 3.90(dd), 4.64(d)
10	Glu	Glutamate	2.05(m), 2.13(m), 2.35(m), 3.76(m)
11	Gln	Glutamine	2.13(m), 2.46(m), 3.77(m)
12	GLT	Glutathione	2.16(m), 2.56 (m), 2.96(m), 3.78(m)
13	GPC	Glycerolphosphocholine	3.23(s), 3.67(dd), 3.88(m), 4.33(m)
14	Gly	Glycine	3.56(s)
15	mI	<i>myo</i> -Inositol	3.28(t), 3.53(dd), 3.62(t), 4.06(t)
16	Lac	Lactate	1.33(d), 4.12(q)
17	Leu	Leucine	0.97(t), 1.72(m), 3.74(t)
18	Lip	Lipid	0.89(t), 1.29(m), 1.69(m), 2.03(m), 2.25(m), 2.77(m)
19	Lys	Lysine	1.48(m), 1.73(m), 1.91(m), 3.03(t), 3.76(t)
20	Pcr	Phosphocreatine	3.04(s)
21	PC	Phosphorylcholine	3.22(s), 3.66(m), 4.30(m)
22	si	<i>scyllo</i> -inositol	3.35(s)
23	Tau	Taurine	3.26(t), 3.43(t)
24	Thr	Threonine	1.34(d), 3.59(d), 4.26(m)

### 2.3 Principal components analysis

Figure 3 showed the PCA results on the brain tumors in the forms of scores plots and loadings plots. The former (Figure 3a) showed that low-grade astrocytomas were well separated from meningiomas. The loadings plot (Figure 3b) showed that the major metabolic differences were highlighted by higher levels of creatine and/or phosphocreatine, GPC, PC and *myo*-inositol in low-grade astrocytomas than in meningiomas, which were confirmed by spectral inspection. One of the meningioma samples (indicated

with an arrow) was clustered with low-grade astrocytomas and close inspection in the third principal component axis showed that this sample was not truly clustered to the low-grade astrocytomas. The spectrum of this sample did, however, show relatively high level of *myo*-inositol, GPC and PC together with low levels of creatine, glutamine and lactate than that of other meningiomas. The reasons for this remain to be understood with limited number of the tumor samples. Histopathological re-examination, nevertheless, confirmed it as a fibroblastic meningioma. The

**Fig. 3** PCA (PC1 vs PC2) plots of 600 MHz HR-MAS <sup>1</sup>H NMR spectra of 39 human brain tumors

Scores plot (a) and loading profile (b), the principal components PC1 and PC2 describe 32% and 22% of variables in the spectra, respectively. ■ : Low-grade astrocytoma; ◇ : Meningioma.

observation of the changes in creatine and/or phosphocreatine suggests that their resonances cannot be used as an internal quantification reference in the tumor studies.

Principal component analysis was also performed on the spectra of 13 fibroblastic and 11 transitional meningiomas. The scores plots (Figure 4a) showed some broad metabonomic differences between fibroblastic and transitional meningiomas; 10 of 13

translational meningiomas were clustered separately from the fibroblastic group. The loadings plot (Figure 4b) showed that  $^1\text{H}$  NMR signals of lactate, glutamate, glutamine, glutathione, and other metabolites including leucine, isoleucine, lysine, glycerolphosphocholine, phosphocholine, glucose ( $\alpha$ -glucose,  $\beta$ -glucose) in the range of region ( $\delta$  3.66~3.90) were lower in fibroblastic meningiomas compared with transitional meningiomas.

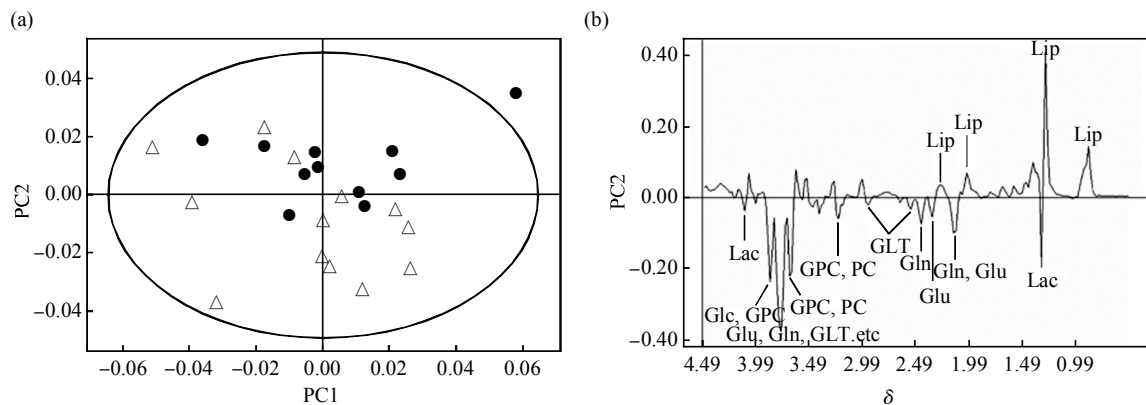


**Fig. 4** PCA (PC1 vs PC2) plots of 600 MHz HR-MAS  $^1\text{H}$  NMR spectra of 24 meningiomas

Scores plot (a) and loading plot (b), the principal components PC1 and PC2 describe 39% and 23% of variables in the spectra, respectively.  $\Delta$  : Fibroblastic meningioma;  $\bullet$  : Transitional meningioma.

## 2.4 Conventional statistical analysis

The above observed metabolite changes were also analyzed by two-tailed student's *t*-test based on the relative concentration from the normalized signal intensities and the results were shown in Figure 5, 6. Apart from statistically significant difference ( $P < 0.05$ ) reported between gliomas and meningiomas in the levels of creatine, *myo*-inositol, glutamate, glutathione, and alanine, this study also observed statistically

significant difference ( $P < 0.05$ ) in the levels of GPC, PC and taurine between low-grade astrocytomas and meningiomas (Figure 5a). Furthermore, significant difference was observed in the level of lipid ( $\delta$  0.89) between fibroblastic and transitional meningiomas (Figure 5b), significant difference can also be found between some metabolite signals at  $\delta$  3.74~3.90 (data not shown), which may partly be attributable to differences in glutathione and glutamate.

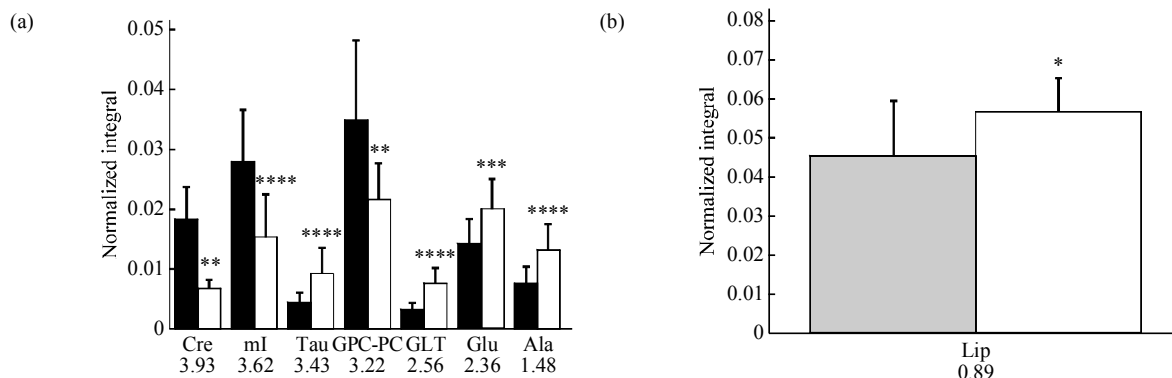


**Fig. 5** Intensities (normalized integral) of some metabolites showing significant differences in different tumors

(a) 15 low-grade astrocytomas and 24 meningiomas.  $\blacksquare$ : Astrocytoma;  $\square$ : Meningioma. (b) 13 fibroblastic meningioma and 11 transitional meningioma.  $\blacksquare$ : Fibroblastic MM;  $\square$ : Transitional MM. \*\*\*\*  $P < 0.0001$ ; \*\*\*  $P < 0.0005$ ; \*\*  $P < 0.005$ ; \*  $P < 0.05$  in *t*-test.

In the literature reported MRS studies, the creatine level was normally used as the internal concentration standard<sup>[46]</sup> assuming its constant concentration in normal brain tissues. However, the level of creatine was found not constant here and in literature<sup>[47]</sup> for the brain tumor tissues. In this study, we found that the level of choline was not statistically different amongst these samples (data not shown), thus the concentration ratios of the observed metabolites against choline (at  $\delta$  3.20) were also calculated and subjected to two-tailed student's *t*-test. Such relative ratios were explored for their significances. Due to signal overlapping ( $\delta$  3.24~3.21)<sup>[48]</sup>, GPC and PC were combined in this study as one indicator to avoid data

overfitting even though curve-fitting methods may be used to resolve them completely. Apart from statistically significant differences ( $P < 0.05$ ) for the ratios of creatine/choline<sup>[27,28]</sup> and *myo*-inositol/choline<sup>[28]</sup> reported between low-grade gliomas and meningiomas, this study also observed that the ratios to choline were all significantly different for taurine, glutathione, glutamate, alanine and the sum of GPC and PC comparing low-grade astrocytomas with meningiomas (Figure 6a). Significant differences in the concentration ratios to choline have also been found for the first time for glutamate between the fibroblastic and transitional meningiomas (Figure 6b).

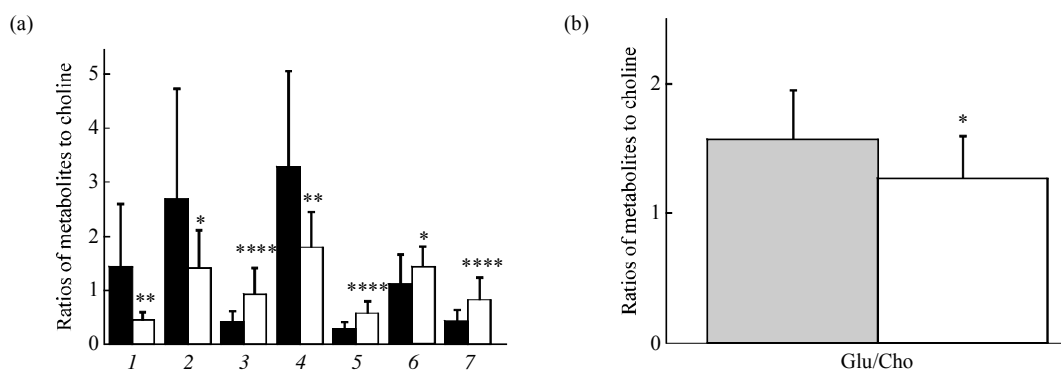


**Fig. 6 The concentration ratios of metabolites to choline showing significant differences in different tumors**

(a) 15 low-grade astrocytomas and 24 meningiomas. 1: Cre/Cho; 2: ml/Cho; 3: Tau/Cho; 4: GPC-PC/Cho; 5: GLT/Cho; 6: Glu/Cho; 7: Ala/Cho. ■: Astrocytoma; □: Meningioma. (b) 13 fibroblastic meningioma and 11 transitional meningioma. ▒: Fibroblastic MM; □: Transitional MM. \*\*\*\*  $P < 0.0005$ ; \*\*\*  $P < 0.005$ ; \*\*  $P < 0.01$ ; \*  $P < 0.05$ , in two-tailed student's *t*-test.

### 3 Discussion

Low level of NAA in low-grade astrocytomas observed here is consistent with what has been observed previously<sup>[13,41]</sup> probably due to the loss of neurons during astrocytomas development as NAA is an important marker of neuron. NAA was not detected in meningiomas probably due to the absence of neurons and axons there. The increase of glutathione was found in meningiomas<sup>[37]</sup> previously probably resulting from the requirement of oxidative stress management during carcinogenesis and development. The observed differences for the levels of glutamine, glutamate, lactate and alanine in low-grade astrocytomas and meningiomas were in good agreement with those from the previous studies<sup>[11, 12, 14, 27, 31, 39]</sup> though glutamine and glutamate were often reported together without resolution. Since glutamate is an excitatory neurotransmitter synthesized

through glutamate dehydrogenase functioning as an  $\alpha$ -ketoglutarate precursor and glutamine is a precursor and storage form of glutamate<sup>[49, 50]</sup>, such observed changes as well as that of glycine are probably related to alterations in the citrate cycle related metabolisms. The increase of alanine level was reported as a specific marker for meningiomas in previous studies<sup>[13,28, 51]</sup>. The differences in the levels of alanine and lactate between low-grade astrocytomas and meningiomas observed here are probably related to the differences in glycolysis<sup>[49]</sup> for these tumors. The higher lactate level in meningiomas than in low-grade astrocytomas was consistent with finding from the previous *ex vivo* studies<sup>[14,41]</sup> though not consistent with that the *in vivo* studies<sup>[27]</sup>. This discrepancy was previously attributed to metabolism during sample preparation and surgical procedures. However, when the metabolite composition was compared under identical conditions during surgical procedures and sample handling in

HRMAS NMR experiments, the lactate differences may also be considered from the differences between tumor tissues. Nevertheless, it cannot be ruled out that poor resolution under *in vivo* MRS studies may also yield some discrepancy. Our observed creatine differences agreed well with the findings in previous studies<sup>[11, 13, 14, 27, 28, 31, 39~41]</sup> in that the level of creatine in human tumors was significantly lower in meningiomas compared with low-grade gliomas. Such changes in creatine level indicate altered energy metabolism in the tumors since creatine is a known reserve for high-energy phosphates and a buffer in adenosine triphosphate and adenosine diphosphate reservoirs<sup>[29, 52]</sup>. Higher level of *myo*-inositol in low-grade astrocytomas has been observed in previous *in vivo* MRS studies<sup>[11, 12, 14, 31, 39, 40]</sup> and *myo*-inositol was identified as a glia-specific marker<sup>[50, 53]</sup>. Observed differences in taurine levels are also consistent with previous observations<sup>[31]</sup>. However, the reasons for the elevation of taurine in meningiomas compared with low-grade astrocytomas were not entirely clear at this stage though osmoregulation and neurotransmitter modulations are primary functions. Synthesized through cysteine, elevation of taurine levels was also related to some cell-damage<sup>[49]</sup>.

Unlike *in vivo* MRS studies where choline, PC and GPC were often reported as “total choline” due to lack of spectral resolution. In this study, GPC and choline or PC and choline in all tumors were well resolved though the peaks of PC and GPC presented partial overlapping. The choline level was not found significantly different between the low-grade astrocytomas and meningiomas whereas the levels of GPC and PC were much higher in low-grade astrocytomas than those in meningiomas. Since choline is a precursor for the biosynthesis of acetylcholine and phosphatidylcholine, the changes in the levels of choline, PC and GPC are probably associated with membrane phospholipid metabolism of tumors<sup>[54, 55]</sup> and related to the tumor cell proliferation. Furthermore, the ratios of a number of metabolites to choline were significantly different between low-grade astrocytomas and meningiomas. The combination of these metabolite/ choline ratios from the HRMAS NMR spectra may have some potential in assisting classification of low-grade astrocytomas and meningiomas. Our observation in the change of lipids was not observed previously. The resonance of lipids in healthy human brain was not normally observable

under *in vivo* MRS conditions and the presence of lipids commonly relate to carcinogenesis. Such increases in lipid levels may accompanied with hypoxia, hypoxic stress, and finally to necrosis as the tumor outgrows its blood supply<sup>[29]</sup>.

In summary, compared with conventional *in vivo* <sup>1</sup>H MRS and *in vitro* <sup>1</sup>H NMR spectroscopy, HRMAS <sup>1</sup>H NMR spectroscopy requires minimal sample preparation and offers more detailed metabolite information. HRMAS <sup>1</sup>H NMR spectroscopy combined with pattern recognition can provide not only important information on relevant metabolites and their ratios for understanding physiology and pathology of the tumors, but also a rapid, nondestructive and accurate way for classification of human brain tumors, which is potentially complementary to the conventional ones. With many more cases studied in the current study, previously reported metabolic differences were further confirmed between low-grade astrocytomas and meningiomas. Some more differences were also observed for the levels of taurine, GPC, PC and lipids.

## References

- 1 Kaibara T, Tyson R L, Sutherland G R. Human cerebral neoplasms studied using MR spectroscopy: a review. *Biochem Cell Biol*, 1998, **76**(2~3): 477~486
- 2 Mainio A, Hakko H, Timonen M, *et al.* Depression in relation to survival among neurosurgical patients with a primary brain tumor: a 5-year follow-up study. *Neurosurgery*, 2005, **56**(6): 1234~1241
- 3 Doolittle N D. State of the science in brain tumor classification. *Semin Oncol Nurs*, 2004, **20**(4): 224~230
- 4 Cheng L L, Ma M J, Becerra L, *et al.* Quantitative neuropathology by high resolution magic angle spinning proton magnetic resonance spectroscopy. *Proc Natl Acad Sci USA*, 1997, **94**(12): 6408~6413
- 5 Devos A, Simonetti A W, van der Graaf M, *et al.* The use of multivariate MR imaging intensities versus metabolic data from MR spectroscopic imaging for brain tumour classification. *J Magn Reson*, 2005, **173**(2): 218~228
- 6 Utriainen M, Komu M, Vuorinen V, *et al.* Evaluation of brain tumor metabolism with <sup>13</sup>C choline PET and <sup>1</sup>H-MRS. *J Neurooncol*, 2003, **62**(3): 329~338
- 7 Roelcke U, Leenders K L. PET in neuro-oncology. *J Cancer Res Clin Oncol*, 2001, **127**(1): 2~8
- 8 Roberts H C, Roberts T P, Lee T Y, *et al.* Dynamic, contrast-enhanced CT of human brain tumors: quantitative assessment of blood volume, blood flow, and microvascular permeability: report of two cases. *AJNR Am J Neuroradiol*, 2002, **23**(5): 828~832
- 9 Zarbo R J, Meier F A, Raab S S. Error detection in anatomic pathology. *Arch Pathol Lab Med*, 2005, **129**(10): 1237~1245
- 10 Takekawa Y, Kinukawa N, Nemoto N, *et al.* Usefulness of cytology applied simultaneously to frozen section at rapid intraoperative

- diagnosis of intracranial tumors. Rinsho Byori, 1998, **46**(9): 954~958
- 11 Majos C, Julia-Sape M, Alonso J, *et al.* Brain tumor classification by proton MR spectroscopy: comparison of diagnostic accuracy at short and long TE. AJNR Am J Neuroradiol, 2004, **25**(25): 1696~1704
  - 12 Tate A R, Majos C, Moreno A, *et al.* Automated classification of short echo time in *in vivo* <sup>1</sup>H brain tumor spectra: a multicenter study. Magn Reson Med, 2003, **49**(1): 29~36
  - 13 Lehnhardt F G, Bock C, Rohn G, *et al.* Metabolic differences between primary and recurrent human brain tumors: a <sup>1</sup>H NMR spectroscopic investigation. NMR Biomed, 2005, **18**(6): 371~382
  - 14 Cheng L L, Chang I W, Louis D N, *et al.* Correlation of high-resolution magic angle spinning proton magnetic resonance spectroscopy with histopathology of intact human brain tumor specimens. Cancer Res, 1998, **58**(9): 1825~1832
  - 15 Martinez-Bisbal M C, Marti-Bonmati L, Piquer J, *et al.* <sup>1</sup>H and <sup>13</sup>C HR-MAS spectroscopy of intact biopsy samples *ex vivo* and *in vivo* <sup>1</sup>H MRS study of human high grade gliomas. NMR Biomed, 2004, **17**(4): 191~205
  - 16 Waters N J, Garrod S, Farrant R D, *et al.* High-resolution magic angle spinning <sup>1</sup>H NMR spectroscopy of intact liver and kidney: optimization of sample preparation procedures and biochemical stability of tissue during spectral acquisition. Anal Biochem, 2000, **282**(1): 16~23
  - 17 Bollard M E, Garrod S, Holmes E, *et al.* High-resolution <sup>1</sup>H and <sup>1</sup>H-<sup>13</sup>C magic angle spinning NMR spectroscopy of rat liver. Magn Reson Med, 2000, **44**(2): 201~207
  - 18 Garrod S, Humphreys E, Connor S C, *et al.* High-resolution <sup>1</sup>H NMR and magic angle spinning NMR spectroscopic investigation of the biochemical effects of 2-bromoethanamine in intact renal and hepatic tissue. Magn Reson Med, 2001, **45**(5): 781~790
  - 19 Valonen P K, Griffin J L, Lehtimäki K K, *et al.* High-resolution magic-angle-spinning <sup>1</sup>H NMR spectroscopy reveals different responses in choline-containing metabolites upon gene therapy-induced programmed cell death in rat brain glioma. NMR Biomed, 2005, **18**(4): 252~259
  - 20 Martinez-Granados B, Monleon D, Martinez-Bisbal M C, *et al.* Metabolite identification in human liver needle biopsies by high-resolution magic angle spinning <sup>1</sup>H NMR spectroscopy. NMR Biomed, 2006, **19**(1): 90~100
  - 21 Cheng L L, Chang I W, Smith B L, *et al.* Evaluating human breast ductal carcinomas with high-resolution magic-angle spinning proton magnetic resonance spectroscopy. J Magn Reson, 1998, **135**(1): 194~202
  - 22 Cheng L L, Wu C, Smith M R, *et al.* Non-destructive quantitation of spermine in human prostate tissue samples using HRMAS <sup>1</sup>H NMR spectroscopy at 9.4 T. FEBS Lett, 2001, **494**(1~2): 112~116
  - 23 Wang Y, Bollard M E, Keun H, *et al.* Spectral editing and pattern recognition methods applied to high-resolution magic-angle spinning <sup>1</sup>H nuclear magnetic resonance spectroscopy of liver tissues. Anal Biochem, 2003, **323**(1): 26~32
  - 24 Cheng L L, Burns M A, Taylor J L, *et al.* Metabolic characterization of human prostate cancer with tissue magnetic resonance spectroscopy. Cancer Res, 2005, **65**(8): 3030~3034
  - 25 Wang Y, Holmes E, Nicholson J K, *et al.* Metabonomic investigations in mice infected with schistosoma *mansonii*: an approach for biomarker identification. Proc Natl Acad Sci USA, 2004, **101**(34): 12676~12681
  - 26 Sitter B, Lundgren S, Bathen T F, *et al.* Comparison of HR MAS MR spectroscopic profiles of breast cancer tissue with clinical parameters. NMR Biomed, 2006, **19**(1):30~40
  - 27 Majos C, Alonso J, Aguilera C, *et al.* Proton magnetic resonance spectroscopy (<sup>1</sup>H MRS) of human brain tumours: assessment of differences between tumour types and its applicability in brain tumour categorization. Eur Radiol, 2003, **13**(3): 582~591
  - 28 Howe F A, Barton S J, Cudlip S A, *et al.* Metabolic profiles of human brain tumors using quantitative *in vivo* <sup>1</sup>H magnetic resonance spectroscopy. Magn Reson Med, 2003, **49**(2): 223~232
  - 29 Tong Z, Yamaki T, Harada K, *et al.* *In vivo* quantification of the metabolites in normal brain and brain tumors by proton MR spectroscopy using water as an internal standard. Magn Reson Imaging, 2004, **22**(7): 1017~1024
  - 30 Roda J M, Pascual J M, Carceller F, *et al.* Nonhistological diagnosis of human cerebral tumors by <sup>1</sup>H magnetic resonance spectroscopy and amino acid analysis. Clin Cancer Res, 2000, **6**(10): 3983~3993
  - 31 Kinoshita Y, Yokota A. Absolute concentrations of metabolites in human brain tumors using *in vitro* proton magnetic resonance spectroscopy. NMR Biomed, 1997, **10**(1): 2~12
  - 32 Tong Z Y, Toshiaki Y, Wang Y J. Proton magnetic resonance spectroscopy of normal human brain and glioma: a quantitative *in vivo* study. Chin Med J (Engl), 2005, **118**(15): 1251~1257
  - 33 Florian C L, Preece N E, Bhakoo K K, *et al.* Characteristic metabolic profiles revealed by <sup>1</sup>H NMR spectroscopy for three types of human brain and nervous system tumours. NMR Biomed, 1995, **8**(6): 253~264
  - 34 Devos A, Lukas L, Suykens J A, *et al.* Classification of brain tumours using short echo time <sup>1</sup>H MR spectra. J Magn Reson, 2004, **170**(1): 164~175
  - 35 Lukas L, Devos A, Suykens J A, *et al.* Brain tumor classification based on long echo proton MRS signals. Artif Intell Med, 2004, **31**(1): 73~89
  - 36 Majos C, Alonso J, Aguilera C, *et al.* Utility of proton MR spectroscopy in the diagnosis of radiologically atypical intracranial meningiomas. Neuroradiology, 2003, **45**(3): 129~136
  - 37 Opstad K S, Provencher S W, Bell B A, *et al.* Detection of elevated glutathione in meningiomas by quantitative *in vivo* <sup>1</sup>H MRS. Magn Reson Med, 2003, **49**(4): 632~637
  - 38 Pfeuffer J, Tkac I, Provencher S W, *et al.* Toward an *in vivo* neurochemical profile: quantification of 18 metabolites in short-echo-time <sup>1</sup>H NMR spectra of the rat brain. J Magn Reson, 1999, **141**(1): 104~120
  - 39 Lehnhardt F G, Rohn G, Ernestus R I, *et al.* <sup>1</sup>H- and <sup>31</sup>P-MR spectroscopy of primary and recurrent human brain tumors *in vitro*: malignancy-characteristic profiles of water soluble and lipophilic spectral components. NMR Biomed, 2001, **14**(5): 307~317
  - 40 Peeling J, Sutherland G. High-resolution <sup>1</sup>H NMR spectroscopy studies of extracts of human cerebral neoplasms. Magn Reson Med, 1992, **24**(1): 123~136
  - 41 Barton S J, Howe F A, Tomlins A M, *et al.* Comparison of *in*

- vivo*  $^1\text{H}$  MRS of human brain tumours with  $^1\text{H}$  HR-MAS spectroscopy of intact biopsy samples *in vitro*. *Magma*, 1999, **8**(21): 121~128
- 42 Farrant R D, Lindon J C, Nicholson J K. Internal temperature calibration for  $^1\text{H}$  NMR spectroscopy studies of blood plasma and other biofluids. *NMR Biomed*, 1994, **7**(5): 243~247
- 43 Nicholls A W, Mortishire-Smith R J. Temperature calibration of a high-resolution magic-angle spinning NMR probe for analysis of tissue samples. *Magn Reson Chem*, 2001, **39**(3): 773~776
- 44 Cheng L L, Lean C L, Bogdanova A, *et al.* Enhanced resolution of proton NMR spectra of malignant lymph nodes using magic-angle spinning. *Magn Reson Med*, 1996, **36**(5): 653~658
- 45 Govindaraju V, Young K, Maudsley A A. Proton NMR chemical shifts and coupling constants for brain metabolites. *NMR Biomed*, 2000, **13**(3): 129~153
- 46 Saunders D E, Howe F A, van den Boogaart A, *et al.* Aging of the adult human brain: *in vivo* quantitation of metabolite content with proton magnetic resonance spectroscopy. *J Magn Reson Imaging*, 1999, **9**(5): 711~716
- 47 Chang L, Ernst T, Osborn D, *et al.* Proton spectroscopy in myotonic dystrophy: correlations with CTG repeats. *Arch Neurol*, 1998, **55**(3): 305~311
- 48 Loening N M, Chamberlin A M, Zepeda A G, *et al.* Quantification of phosphocholine and glycerophosphocholine with  $^{31}\text{P}$  edited  $^1\text{H}$  NMR spectroscopy. *NMR Biomed*, 2005, **18**(7): 413~420
- 49 Zwingmann C, Leibfritz D. Regulation of glial metabolism studied by  $^{13}\text{C}$ -NMR. *NMR Biomed*, 2003, **16**(6~7): 370~399
- 50 Ross B D. Biochemical considerations in  $^1\text{H}$  spectroscopy. Glutamate and glutamine; *myo*-inositol and related metabolites. *NMR Biomed*, 1991, **4**(2): 59~63
- 51 Hazany S, Hesselink J R, Healy J F, *et al.* Utilization of glutamate/creatine ratios for proton spectroscopic diagnosis of meningiomas. *Neuroradiology*, 2007, **49**(2): 121~127
- 52 Kreis R, Ernst T, Ross B D. Development of the human brain: *in vivo* quantification of metabolite and water content with proton magnetic resonance spectroscopy. *Magn Reson Med*, 1993, **30**(4): 424~437
- 53 Brand A, Richter-Landsberg C, Leibfritz D. Multinuclear NMR studies on the energy metabolism of glial and neuronal cells. *Dev Neurosci*, 1993, **15**(3~4): 289~298
- 54 Podo F. Tumour phospholipid metabolism. *NMR Biomed*, 1999, **12**(7): 413~439
- 55 Yang Y X, Li C L, Nie X, *et al.* Metabonomic studies of human hepatocellular carcinoma using high-resolution magic-angle spinning  $^1\text{H}$  NMR spectroscopy in conjunction with multivariate data analysis. *J Proteome Res*, 2007, **6**(7): 2605~2614

## 高分辨魔角旋转核磁共振和主成分分析研究人类 低级星形细胞瘤和脑膜瘤的代谢组特征\*

陈文学<sup>1,2)</sup> 楼海燕<sup>3,4)</sup> 张红萍<sup>5)</sup> 聂秀<sup>6)</sup> 向云<sup>1,2)</sup> 杨永霞<sup>1,2)</sup> 吴光耀<sup>1,5)</sup>  
漆剑频<sup>3)</sup> 岳勇<sup>1)</sup> 雷皓<sup>1)</sup> 唐惠儒<sup>1)\*\*</sup> 邓风<sup>1)\*\*</sup>

<sup>1)</sup>中国科学院武汉物理与数学研究所, 波谱与原子分子物理国家重点实验室, 武汉 430071; <sup>2)</sup>中国科学院研究生院, 北京 100049;

<sup>3)</sup>华中科技大学同济医学院, 同济医院, 武汉 430022; <sup>4)</sup>浙江大学医学院附属第一医院, 杭州 310003;

<sup>5)</sup>武汉大学医学院, 中南医院, 武汉 430071; <sup>6)</sup>华中科技大学同济医学院, 协和医院, 武汉 430022)

**摘要** 采用高分辨魔角旋转核磁共振(HRMAS  $^1\text{H}$  NMR)技术结合主成分分析(PCA)方法研究了 39 例人体脑肿瘤组织的代谢组特征。39 例肿瘤样本分别来自 39 个脑肿瘤患者, 包括 15 例低级星形细胞瘤, 13 例纤维型脑膜瘤和 11 例过渡型脑膜瘤。核磁共振波谱分析结果表明, 脑肿瘤组织的代谢组中主要含有脂肪酸、乳酸、胆碱代谢物(如胆碱、磷酸胆碱和甘油磷酸胆碱)、氨基酸(如丙氨酸、谷氨酸、谷氨酰胺、牛磺酸)、N-乙酰天门冬氨酸(NAA)和谷胱甘肽等代谢物。通过对核磁共振谱进行主成分分析(PCA), 发现低级星形细胞瘤和脑膜瘤的代谢组之间具有明显的差异, 而在过渡型和纤维型两个亚类脑膜瘤之间该差别相对较小。与脑膜瘤相比, 低级星形细胞瘤中甘油磷酸胆碱、磷酸胆碱、肌醇与肌酸的含量较高, 而丙氨酸、谷氨酸、谷氨酰胺、谷胱甘肽和牛磺酸的含量较低。NAA 的含量在低级星形细胞瘤中尽管较低但能观察到, 而脑膜瘤中却未发现 NAA 的信号。结果表明, HRMAS  $^1\text{H}$  NMR 和多变量统计分析相结合的组织代谢组学方法, 不仅能有效区分不同类型的脑肿瘤, 而且还可以为脑肿瘤提供丰富的代谢组信息, 这些信息对研究肿瘤发生发展的机制具有潜在的意义。

**关键词** 脑肿瘤, 胶质瘤, 星形细胞瘤, 脑膜瘤, 高分辨魔角旋转核磁共振, 模式识别, 统计分析

**学科分类号** R73, O65

\* 国家自然科学基金(10234070, 20573132 和 20575074)和中国科学院“百人计划”(T12508-06S138)资助项目。

\*\* 通讯联系人. Tel: 027-87198430, 027-87198820

唐惠儒. E-mail: Huiru.Tang@wipm.ac.cn

邓风. E-mail: Dengf@wipm.ac.cn

收稿日期: 2008-01-28, 接受日期: 2008-04-15